Chitosan-elicited defense responses in Cucumber mosaic virus (CMV)-infected tomato plants

Peer-reviewed author version

Rendina, Nunzia; Nuzzaci, Maria; Scopa, Antonio; CUYPERS, Ann & Sofo, Adriano
(2019) Chitosan-elicited defense responses in Cucumber mosaic virus (CMV)-infected tomato plants. In: Journal of Plant Physiology, 234, p. 9-17.

DOI: 10.1016/j.jplph.2019.01.003
Handle: http://hdl.handle.net/1942/29729

Chitosan-elicited defense responses in *Cucumber mosaic virus* (CMV)-infected tomato plants

Nunzia Rendina[a*], Maria Nuzzaci[a], Antonio Scopa[a], Ann Cuypers[b], Adriano Sofo[a]

[a] School of Agricultural, Forestry, Food and Environmental Sciences, University of Basilicata, Viale dell' Ateneo Lucano, 10, 85100 Potenza, Italy
[b] Environmental Biology, Centre for Environmental Sciences, Hasselt University, Agoralaan, Building D, 3590 Diepenbeek, Belgium

[*] Corresponding author: nunzia.rendina@unibas.it (Nunzia Rendina) School of Agricultural, Forestry, Food and Environmental Sciences, University of Basilicata, Viale dell' Ateneo Lucano, 10, 85100 Potenza, Italy

nunzia.rendina@unibas.it (Nunzia Rendina); maria.nuzzaci@unibas.it (Maria Nuzzaci); antonio.scopa@unibas.it (Antonio Scopa); ann.cuypers@uhasselt.be (Ann Cuypers); adriano.sofo@unibas.it (Adriano Sofo)

Abbreviations: *A*, photosynthetic activity; ANOVA, analysis of variance; AR156, *Bacillus cereus* AR156; CERK1, chitin elicitor receptor kinase 1; CHT, chitosan; CMV, *Cucumber mosaic virus*; DAS-ELISA, double-antibody sandwich enzyme-linked immunosorbent assay; ET, ethylene; F_v/F_m, maximum quantum yield of PSII; GAPDH, glyceraldehyde-3-phosphate dehydrogenase; g_s, stomatal conductance to water vapor; ISR, induced systemic resistance; JA, jasmonic acid; NPR1, non-expressor of pathogenesis-related genes 1; ϕPSII, quantum yield of PSII; PAL, phenylalanine ammonia lyase; PAR, photosynthetically active radiation; PR, pathogenesis-related; PSY, phytoene synthase; PVX, *Potato virus X*; qPCR, Real-Time quantitative PCR; ROS, reactive oxygen species; SA, salicylic acid; SAR, systemic acquired resistance; TMV, *Tobacco mosaic virus*; TP, treated plants; TUB, tubulin; UK, uridylate kinase

ABSTRACT

The control of plant diseases by inducing plant resistance responses represents an interesting solution to avoid yield losses and protect the natural environment. Hence, the intertwined relationships between host, pathogen and inducer are increasingly subject of investigations. Here,

we report the efficacy of chitosan-elicited defense responses in *Solanum lycopersicum* var. *cerasiforme* plants against *Cucumber mosaic virus* (CMV). Chitosan was applied via foliar spray before the CMV inoculation to verify its effectiveness as a preventive treatment against the viral infection. Virus accumulation, photosynthetic performance, as well as genes encoding for proteins affecting resistance responses and biosynthetic pathways, were investigated. It was observed a significant reduction of CMV accumulation in chitosan-treated plants that were successively infected with CMV, compared to only CMV-infected ones (up to 100%). Similarly, a positive effect of chitosan on gas exchange dynamics was revealed. The analysis of gene expression (*CEVI-1*, *NPR1*, *PSY2* and *PAL5*) suggested the occurrence of chitosan-induced, systemic acquired resistance-related responses associated with a readjustment of the plant's oxidative status. In addition, the absence of deleterious symptoms in chitosan-treated successively CMV-infected plants, confirmed that chitosan can be used as a powerful control agent. Our data indicate that chitosan, when preventively applied, is able to elicit defense responses in tomato to control CMV infection. Such finding may be recommended to protect the tomato fruit yields as well as other crops.

Keywords: Chitosan; *Cucumber mosaic virus*; Defense/antioxidant-related protein; Disease control; Photosynthetic performance; *Solanum lycopersicum* var. *cerasiforme*.

1 Introduction

Plants are susceptible to numerous pathogens responsible for diseases that can reduce crop yield (e.g., (Vitti et al., 2015)), causing severe economic losses. Among the most dangerous phytopathogens, viruses cannot be faced by using specific agrochemicals (Iriti and Varoni, 2015).

Hence, control of viral infections, protecting the natural environment, is the best strategy to ensure an, at least, satisfactory harvest. In such a scenario, elicitors triggering plant defense responses and inducing a systemic resistance state can represent a solution.

Chitosan (CHT) is a polycationic heteropolysaccharide composed by N-acetyl-D-glucosamine and D-glucosamine linked by β-(1→4) glycosidic bonds (Iriti and Varoni, 2015). Although CHT is a natural compound (present in Zygomycetes), it is mainly obtained by the deacetylation of chitin, a component of the fungal cell wall and the arthropod exoskeleton (Iriti and Varoni, 2015). Chitosan polymers may vary in molecular weight, viscosity, pKa value, polymerization and deacetylation degree, affecting their physicochemical and biological properties (Iriti and Varoni, 2015). Chitosan is a biodegradable and nontoxic compound inducing systemic acquired resistance (SAR) to pathogens in plants (Xing et al., 2015). This compound also exhibits a direct antimicrobial activity, likely mainly through electrostatic interactions (Xing et al., 2015). Chitosan bioactivities can be explained because the polycationic nature of CHT leads to affinity with the anionic contents of target organism (Kumaraswamy et al., 2018). More specifically, as an antimicrobial, CHT interaction with cell wall and cell membranes can destabilize them. In addition, its interaction with DNA and proteins can interfere with the transcription and translation mechanisms (Kumaraswamy et al., 2018). Furthermore, CHT can chelate essential nutrients, trace elements and metal ions that are necessary for the microbial growth, as well as it can form a polymer film that compromises metabolite excretion and nutrient uptake (Xing et al., 2015). However, the detailed mechanism of action of CHT in reducing plant diseases has not been completely revealed (Hassan and Chang, 2017). Chitosan perception by plant is shortly followed by a vatiation in the ion fluxes and membrane depolarization (Iriti and Varoni, 2015). Therefore, CHT can be recognized by plant as a pathogen-mimicking stimulus, but the identification of a CHT receptor is still doubtful (Malerba and Cerana, 2016; Povero et al., 2011). Although Petutschnig et al. (2010) found that the chitin elicitor receptor kinase 1 (CERK1) also bound more weakly to CHT, later Povero et al. (2011)

83 demonstrated that the perception of CHT was independent of CERK1. Recently, Liu et al. (2018)
84 suggested wheat W5G2U8,W5HY42, and W5I0R4 as potential chitosan oligosaccharides receptors.
85 Interestingly, the application of CHT to promote the plant growth has also been studied
86 (Kumaraswamy et al., 2018; Sharif et al., 2018) and CHT nanoparticles can also be used to deliver
87 pesticides, herbicides, fertilizers, micronutrients as well as genetic material (Malerba and Cerana,
88 2016). The antimicrobial activity of CHT has been studied for bacteria, yeasts and moulds (Liu et
89 al., 2004). Furthermore, CHT is effective as an alternative treatment to conventional fungicides
90 aimed to control the postharvest decay, both after preharvest (Feliziani et al., 2015) and postharvest
91 applications. The latter is associated with CHT coating of fruits (Sivakumar et al., 2016). On cherry
92 tomato fruit, CHT exerted an inhibitive action on the gray mold (*Botrytis cinerea*), presumably
93 involving the mitogen-activated protein kinase signaling pathway and determining an increase of
94 hydrogen peroxide, peroxidase activity, as well as *PR1a1* and *PR5* transcripts (Zhang et al., 2015).
95 Chitosan-induced responses against viruses, such as *Potato virus X* (PVX) and *Tobacco mosaic*
96 *virus* (TMV), were also evaluated (Chirkov et al., 2001; Jia et al., 2016; Nagorskaya et al., 2014).
97 *Cucumber mosaic virus* (CMV) (genus *Cucumovirus*, family *Bromoviridae*) presents polyhedral
98 virions composed of 180 subunits (T=3 icosahedral symmetry) (Gallitelli, 1998). Virus particles are
99 isometric: separate particles separately contain RNA1 and RNA2, a third particle contains RNA3
100 and subgenomic RNA4 (Agrios, 1997) and possibly RNA3 and subgenomic RNA4A (Gallitelli,
101 2000). RNA1 and RNA2 code for two different proteins involved in RNA replication (Agrios,
102 1997). The 2b protein is translated from the RNA4A of RNA2 (Gallitelli, 2000). RNA3 encodes a
103 protein involved in virus movement and contains the open reading frame for the coat protein. The
104 coat protein cistron is translated via the RNA4 (Gallitelli, 2000). In order to infect plants, the co-
105 infection with the three particles together is required (Gallitelli, 1998). The numerous strains
106 belonging to CMV differ in properties and characteristics such as host plants, symptoms produced,
107 ways of transmission (Agrios, 1997). Infecting at least 100 plant families and 1,200 species

(Edwardson and Christie, 1991), CMV has a wide range of hosts, such as ornamentals and many species of vegetables (Agrios, 1997). Furthermore, CMV causes distortion and discoloration of leaves, fruits and flowers, reduction in quantity and quality of crop yield, up to reduced growth and plant death (Agrios, 1997). It is known that about 80 species of aphids can represent vectors of CMV. For this reason, control approaches can include the removal of aphids and the destruction of CMV reservoirs weeds (Gallitelli, 1998). Interestingly, CMV, *Alfalfa mosaic alfamovirus* (AMV), *Potato M carlavirus* (PVM), *Potato Y potyvirus* (PVY) and *Tomato spotted wilt tospovirus* (TSWV) often compose mixed infections in tomato cultivated in the Mediterranean basin (Gallitelli, 1998). Limited information has been reported on the tools and mechanisms controlling the virus diseases, especially regarding the economically relevant CMV. Specifically, a gap exists in the complete understanding of the tomato-CMV-CHT interaction. For this reason, the viral titer, the plant photosynthetic performance and the expression of genes related to antioxidant compounds and plant resistance responses to pathogens, were investigated in tomato plants infected with CMV, with and without CHT treatment. Therefore, the aim of this work was to investigate the efficacy of CHT as an innovative and eco-friendly strategy to elicit defense responses in tomato plants against CMV, so avoiding the negative consequences of the viral infection.

2 Materials and methods

2.1 Chitosan (CHT) and CMV sources and preparations

Low molecular weight CHT (50-190 kDa, 75-85% deacetylated) was purchased from Sigma-Aldrich (448869; St. Louis, MO, USA). Chitosan (1 g) was dissolved in distilled water (40 mL) containing 1 M acetic acid (9 mL) under overnight continuous stirring. The pH was 5.4. Eliciting CHT solution was prepared by dissolving 1 g of this stock in 1 L of distilled water and foliar

sprayed (10 mL plant^{-1}), while water was sprayed on untreated plants. Obtained as reported by Vitti et al. (2015), *Cucumber mosaic virus* strain Fny inducing necrosis (CMV-Fny) was propagated in *Nicotiana tabacum* cv Xanthi plants. Subsequently, tobacco leaves exhibiting CMV-Fny symptoms were macerated in 0.05 M sodium citrate buffer (pH 6.5) and the suspension was mechanically rubbed on celite pre-dusted tomato leaves.

2.2 Experimental setup

Solanum lycopersicum var. *cerasiforme* seeds were sterilized (1 min in 1% Na-hypochlorite solution) and then put to germinate on moist filter paper imbibed with sterile distilled water in Petri dishes. After incubation for 24 h at 4 °C in the dark and for 2-3 days at 26 °C, seedlings were transferred to pots filled with sterilized soil. At the four-leaf stage, plants were transplanted and grown in a greenhouse at a temperature regime of 26/23 °C (day/night) and with a 16-h photoperiod.

The experimental design included four experimental conditions (15 plants for each condition): untreated plants; plants inoculated with CMV (CMV-TP); plants treated with CHT (CHT-TP); plants treated with CHT and then inoculated with CMV 24 h after CHT treatment (CHT-CMV-TP). Treatment/inoculation was performed starting from the tenth day after transplantation.

2.3 CMV determination

Twenty and ninety days after CMV inoculation, leaves from three plants randomly chosen, were collected and used for a double-antibody sandwich enzyme-linked immunosorbent assay (DAS-ELISA) according to Vitti et al. (2016). Measurements were performed spectrophotometrically

(model Multiskan GO: Thermo Fisher Scientific, Waltham, MA, USA) and the mean absorbance value ($OD_{405\ nm}$) of six replicates for each experimental condition was taken.

2.4 Gas exchange and chlorophyll fluorescence

Photosynthetic activity (A), stomatal conductance to water vapor (g_s), maximum quantum yield of PSII (F_v/F_m) (dark-adapted state) and quantum yield of PSII (ϕPSII) (light-adapted state) were measured on clear days. Two apical fully developed leaves, belonging to one of three (for A and g_s determinations) or of two (for F_v/F_m and ϕPSII determinations) 2- and 4-month-old plants randomly chosen for each experimental condition, were tested. Measurements were carried out using the LI-6400 portable photosynthesis system (LI-COR, Lincoln, NE, USA), operating between 10:00 and 12:00 a.m., at 398 ppm external CO_2 concentration, flow rate at 500 μmol s^{-1} and 1500 μmol photons m^{-2} s^{-1} photosynthetically active radiation (PAR). Temperature inside the leaf chamber was maintained equal to environmental air temperature (28 °C) by instrument automatic temperature regulation.

The same plants used for gas exchange measurements were chosen to measure chlorophyll fluorescence at 10:00-12:00 a.m. using a leaf chamber fluorometer (LI-6400-40; Li-Cor, Inc.). On each plant, both sun-adapted and dark-adapted leaves were chosen to measure fluorescence parameters. On dark-adapted leaves (covered by silver film for 18 h before the measurements by homemade clip holders), the maximum quantum yield of PSII photochemistry was calculated as $F_v/F_m = (F_m - F_o)/F_m$ (Murchie and Lawson, 2013), where F_m is the maximum fluorescence in the dark and F_o is the minimum level of fluorescence. On sun-adapted leaves, the quantum yield of PSII (ϕPSII) was calculated as $(F_m' - F')/ F_m'$ (Murchie and Lawson, 2013), where F_m' is the maximum fluorescence in the light and F' is the steady-state fluorescence yield measured under actinic light. The value of PAR inside the leaf chamber (light with a 90% red fraction at a wavelength of 630 nm

and a 10% blue fraction at 470 nm) during fluorescence measurements was 950 µmol m^{-2} s^{-1}. This value was chosen keeping into account (1) the measured average light saturation point (900 to 1000 µmol m^{-2} s^{-1}) and (2) the mean environmental irradiance monitored by the LI–6400 external quantum light sensor every 3 seconds.

2.5 SPAD measurements

Leaf chlorophyll content was measured with a portable meter (SPAD-502, Minolta Camera Co. Ltd., Osaka, Japan) between 10:00 and 11:00 a.m. Three apical fully developed leaves, belonging to one of two 2- and 4-month-old plants randomly chosen for each condition were tested. The mean value of the six measurements was recorded.

2.6 Extraction and determination of total phenolic content

Extractions and determinations were carried out in two randomly chosen plants for each condition, analyzing leaves collected 60 h after the only or last treatment/inoculation. The total phenolic content was analyzed spectrophotometrically using the Folin-Ciocalteu reagent and catechol as standard, as reported by Sofo et al. (2017). All values were expressed as mg catechol equivalents 100 g^{-1} of leaves fresh weight. The mean absorbance value ($OD_{650\ nm}$) of four replicates for each condition was taken.

2.7 Gene expression analysis

Frozen leaves collected nine days after the only or last treatment/inoculation, from one of four 1.5-month-old plants for each experimental condition, were ground in liquid nitrogen in a

206 pestle and mortar. From the powder obtained, RNA was extracted using the RNAqueous Total RNA
207 Isolation kit (AM1912, Ambion, Life Technologies, Thermo Fisher Scientific, Waltham, MA,
208 USA). On ice, RNA was purified adding 1/10 volume of 3M sodium acetate and 7/10 volume of
209 100% isopropanol. Samples were stored at −80 °C for 30 min, then centrifuged at 4 °C for 15 min
210 at maximum speed. To the pellet saved, 400 µL of 70% ethanol was added and two centrifugations
211 at 4 °C for 2 min at maximum speed taking off the supernatant were carried out. The open tubes
212 were put at 37 °C for 5 min in a heat block (ThermoStat Plus, Eppendorf, Hamburg, Germany) and
213 finally, RNase-free water was added to dissolve the RNA pellet. Purified RNA concentration and
214 purity were spectrophotometrically determined at 260 nm (NanoDrop ND-1000 UV/Vis
215 Spectrophotometer, NanoDrop Technologies, Wilmington, DE, USA). The Experion RNA StdSens
216 Analysis Kit (Bio-Rad Laboratories, Hercules, CA, USA) was used to assess the RNA quality. To
217 the same concentration (1 µg) of all the RNA samples then utilized for the reverse transcription,
218 DNase (TURBO DNA-free Kit, AM1907, Invitrogen, Thermo Fisher Scientific, Waltham, MA,
219 USA) was added to degrade contaminating gDNA. cDNA synthesis was carried out starting from
220 oligo(dT)-primers and random hexamers (PrimeScript RT Reagent Kit, Perfect Real Time,
221 RR037A, Takara, Japan), then the cDNA obtained was 10-fold diluted using 1/10 TE buffer (1 mM
222 Tris-HCl, 0.1 mM EDTA, pH 8.0). Real-Time quantitative PCR (qPCR) was performed
223 coupled with SYBR Green fluorescent dye, using the 7500 Real-Time PCR System (Applied
224 Biosystems, Lennik, Belgium). Cycling conditions were 95 °C for 20 s, 50 cycles of 3 s at 95 °C
225 and 30 s at 60 °C. A final volume of 10 µL contained 2 µL of cDNA produced, 5 µL of Fast SYBR
226 Green Master Mix (4385612, Applied Biosystems, Lennik, Belgium), 0.3 µL of each forward and
227 reverse primer (300 nM) (Table 1) and 2.4 µL of RNase-free water. A dissociation curve followed
228 to evaluate the amplification specificity. Sequences for the reference genes, as well as for the genes
229 of interest, were searched in the NCBI (https://www.ncbi.nlm.nih.gov) and JGI Phytozome
230 (https://phytozome.jgi.doe.gov/pz/portal.html) databases, and related primers were designed using

Primer3 Program and nBLAST-NCBI (Table 1). Primers efficiency ($E = 10^{(-1/slope)} - 1$) was measured using serial dilutions from 1/2 to 1/64 of cDNAs collected in a pooled sample and realizing C_q versus log(dilution) calibration lines (Table 2). The GrayNorm algorithm (https://github.com/gjbex/GrayNorm) was adopted to select the combination of reference genes able to yield the highest possible accuracy. The expression of the genes encoding (EC 1.11.1.7) peroxidase (*CEVI-1*), non-expressor of pathogenesis-related genes 1 (*NPR1*), (EC 2.5.1.32) phytoene synthase 2 (*PSY2*) and (EC 4.3.1.5) phenylalanine ammonia lyase (*PAL5*) was considered relative to five reference genes selected for normalization: *SAND*, *TIP4*, *TUB* (tubulin), *UK* (uridylate kinase) and *GAPDH* (glyceraldehyde-3-phosphate dehydrogenase). In Tables 1 and 2 are respectively reported sequences and efficiencies of primers for the reference genes and genes of interest for qPCR analysis. Genes of interest relative expression was calculated as $2^{-\Delta Cq}$, and the $2^{-\Delta Cq}$ values geometric average was used for data normalization.

254 Table 1 - Primers sequence

Name	Sequence	Tm (°C)
SAND	5'-CCAGCTAACTTTCTCCATGCTTAC-3'	58.1
	5'-ACCAACAAGACTGATAACCTTTTGT-3'	55.3
TIP4	5'-CTGTTAAAGTGAGAGTCATGCCTAG-3'	58.4
	5'-TGCAAACGAGTGTCTCTTAGTCT-3'	57.8
TUB	5'-AGAATGCCGATGAATGTATGGT-3'	55.0
	5'-CAGGGAATCTCAAACAGCAAG-3'	55.2
UK	5'-TGGTAAGGGCACCCAATGTGCTAA-3'	59.7
	5'-ATCATCGTCCCATTCTCGGAACCA-3'	59.9
GAPDH	5'-GATGTCTCCGTTGTCGATCTT-3'	55.1
	5'-CAAGATACCCTTCAATTTACCCTCT-3'	55.9
CEVI-1 (GenBank accession number Y19023)	5'-TCACCAACAAGGGAATGGAT-3'	52.0
	5'-TGGATCAGGGCTACCACTTC-3'	54.9
NPR1 (Phytozome Solyc07g040690.2)	5'-CGATGATTTGCGTATGAAGC-3'	54.3
	5'-CCAGGGGTAATTCAGACGTG-3'	54.4
PSY2 (Phytozome Solyc02g081330.2)	5'-CCGAATTCCGAGGTCTCATA-3'	54.5
	5'-CCTGTCTCCCACCTTTCTTG-3'	54.5
PAL5 (GenBank accession number M90692)	5'-CTCTGGCAATGGGTGCTAAT-3'	55.2
	5'-CAGGGGTCATCAGCATAGGT-3'	55.3

255

256

257

258

259

260

Table 2 - Primers efficiency

Primer	PCR efficiency (80-120%)	Equation	R^2 Coefficient
SAND	93.03%	y = −3.5010x + 25.795	$R^2 = 0.9923$
TIP4	100.51%	y = −3.3097x + 24.447	$R^2 = 0.9964$
TUB	100.78%	y = −3.3035x + 23.606	$R^2 = 0.9984$
UK	87.58%	y = −3.6605x + 25.201	$R^2 = 0.9987$
GAPDH	96.92%	y = −3.3981x + 21.682	$R^2 = 0.9992$
CEVI-1	105.70%	y = −3.1926x + 25.276	$R^2 = 0.9944$
NPR1	103.53%	y = −3.2401x + 25.306	$R^2 = 0.9997$
PSY2	92.89%	y = −3.5049x + 24.470	$R^2 = 0.9939$
PAL5	100.73%	y = −3.3045x + 22.149	$R^2 = 0.9990$

2.8 Statistical data analysis

Normal distribution of data was tested performing the Shapiro-Wilk test ($P \leq 0.05$) and homoscedasticity was tested performing the Bartlett's test ($P \leq 0.05$). Data were analyzed by one- and two-way analysis of variance (ANOVA). Parametric and non-parametric as multiple comparisons were performed using the Tukey's HSD test and the Kruskal-Wallis test, respectively. Statistical analyses were performed using the software RStudio: Integrated Development for R, version 1.0.136 (RStudio, Inc., Boston, MA, USA).

3 Results

Twenty days after CMV inoculation, only CMV-TP showed mosaic and chlorosis in leaves, as well as their deformation (Figure 1A). On the contrary, the absence of symptoms induced by CMV was

277 detected in CHT-CMV-TP (Figure 1A). Furthermore, the same four experimental conditions, with
278 the same inoculations and treatments methods, were also applied to *Nicotiana tabacum*. Eleven
279 days after CMV inoculation, tobacco CMV-TP showed mosaic in leaves, but the absence of CMV
280 symptoms was detected in tobacco CHT-CMV-TP (Figure 1B).
281
282 **3.1 CMV load**
283
284 CHT-CMV-TP showed the mean optical density value significantly lower than that determined in
285 CMV-TP, both in 20 days and 90 days after CMV inoculation determinations (−86% and −100%,
286 respectively). The absence of CMV was detected in untreated and CHT-TP, and no significant
287 difference was revealed between these two conditions (Figure 2).
288
289 **3.2 Gas exchange and chlorophyll fluorescence**
290
291 Considering the *A* value between 2- and 4-month-old plants, CMV-TP and CHT-TP showed the
292 lowest and the highest *A* value, respectively (Figure 3A). Although not significantly, CHT-CMV-
293 TP had the *A* value of 44% higher than that determined in CMV-TP, and untreated plants showed
294 the *A* value lower (−25%) than that determined in CHT-TP (Figure 3A). The 2-month-old CHT-TP
295 and CMV-TP showed the highest and the lowest g_s value, respectively (Figure 3B). Chitosan
296 treatment in CHT-CMV-TP caused a g_s value of 146% significantly higher than that determined in
297 CMV-TP, and a g_s value not significantly different than that determined in CHT-TP. Untreated
298 plants showed a g_s value not significantly different than that of CMV-TP, and a g_s value
299 significantly lower (−59%) than that of CHT-TP (Figure 3B). Results were not significantly
300 different between the four conditions, in 4-month-old plants (Figure 3B). The 4-month-old CHT-TP
301 and CHT-CMV-TP showed a significant decrease in the g_s value, compared to the g_s value of 2-

month-old plants (−58 and −50%, respectively) (Figure 3B). The 4-month-old CMV-TP showed the lowest F_v/F_m value, lower (−6%) than the average value of the F_v/F_m values of all the other conditions (Figure 3C). The 4-month-old CMV-TP also showed a significant decrease of the F_v/F_m value, compared to that determined in 2-month-old plants (−7%) (Figure 3C). The 4-month-old untreated, CHT-TP and CHT-CMV-TP showed a significant increase in the ϕPSII value, compared to that of 2-month-old plants (298, 217 and 218%, respectively) (Figure 3D).

3.3 SPAD

In 2-month-old plants, CHT-TP had a SPAD value 11% significantly higher than that found in untreated plants. Finally, among 4-month-old plants, the CHT-CMV-TP showed the lowest SPAD value (Figure 4).

3.4 Total phenolic content

Untreated plants and CHT-CMV-TP showed the highest and the lowest total phenolic content, respectively. CHT-CMV-TP showed a total phenolic content significantly lower than that determined in untreated and CMV-TP (−41 and −40%, respectively) (Figure 5).

3.5 Gene expression analysis

Reference genes were TUB, UK and GAPDH for the experimental conditions represented in Figure 6; SAND, TIP4 and GAPDH for those represented in Figure 7.

Untreated plants were assumed as a control, compared to CMV-TP, and no significant difference was found in the relative expression of all the genes of interest assayed (Figure 6). Although not

significant, an increase in *CEVI-1* transcripts was detected in the leaves of CMV-TP (Figure 6A). Finally, *PAL5* expression was the most stable in the considered conditions (Figure 6).

CMV-TP were then assumed as a control, compared to CHT-TP and CHT-CMV-TP (Figure 7). A significant increase in *PAL5* expression was observed both in CHT-TP and CHT-CMV-TP, compared to CMV-TP (Figure 7D). Conversely, no significant up-regulation of *NPR1* and down-regulation of *CEVI-1* and *PSY2* transcripts were observed (Figures 7B, A and C, respectively).

4 Discussion

The plant-virus interaction affects the chloroplast. More specifically, the virus replication and viral movement involve chloroplast factors (Zhao et al., 2016). As a result, the chloroplast structure and the expression of photosynthesis-related proteins are perturbed as well as the viral symptoms are manifested (Zhao et al., 2016).

Studies have shown the efficacy against strains of CMV infection of treatment with *Trichoderma harzianum* T-22 (Vitti et al., 2016, 2015), *Paenibacillus lentimorbus* B-30488 (Kumar et al., 2016) and benzo-(1,2,3)-thiadiazole-7-carbothioic acid *S*-methyl ester (BTH) (Anfoka, 2000).

The present research investigated the ability of CHT to elicit defense response in tomato plants inoculated with CMV.

4.1 CMV symptoms and load monitoring

A phenotypical observation showed the capacity of CHT to control CMV symptoms, testing tomato and tobacco as host plants. Indeed, neither tomato nor tobacco CHT-treated then CMV-infected plants displayed viral infection symptoms (Figures 1A and B, respectively). The results of DAS-

ELISA showed the efficacy of CHT to control foliar CMV load in tomato CHT-CMV-TP, both at 20 days and at 90 days after CMV inoculation measurements (Figure 2). In agreement with our results, determined by ELISA, a CHT-induced resistance in potato against PVX was suggested as probably mediated by the enhanced ribonuclease activity and callose deposition (Chirkov et al., 2001). Furthermore, in *Nicotiana tabacum* L. cv. Samsun leaves, Nagorskaya et al. (2014) showed that CHT limited TMV coat protein content and infectivity as well as increased the hydrolases (proteases and RNases) activity. They also detected a highest content of abnormal virions.

4.2 Plant physiological responses to CHT and CMV

Photosynthetic activity was considerably analogous, between the short and long term (when plants were 2- and 4-month-old, respectively). Although not significantly, CHT treatment improved the photosynthetic activity (Figure 3A). Van et al. (2013) reported the effects of CHT nanoparticles on Robusta coffee and, according to our results, they found an enhanced photosynthesis net rate and besides, they supposed increased stomatal cells opening degree and stomatal conductance because of the polycation property of CHT that raise the osmosis pressure of stomatal cells. Salachna et al. (2017) suggested that the positive effect of CHT on plant growth parameters may cause the increased stomatal conductance with CHT foliar application. However, the reduction of stomatal apertures width after foliar CHT treatment of bean has also been reported (Iriti et al., 2009). Differently from *A* data, effect of treatment/inoculation on stomatal conductance was more evident when plants were 2-month-old (Figure 3B). As reported by Vitti et al. (2016), the 2-month-old tomato plants inoculated with CMV showed reduced stomatal conductance to water vapor besides decreased photosynthetic activity (Figures 3B and A, respectively).

374 In agreement with the results obtained by Marler et al. (1993) on papaya leaves inoculated with
375 *Papaya ringspot virus* (PRV), a significantly lower maximal quantum yield of PSII value (F_v/F_m)
376 was detected in CMV-TP than untreated ones, in 4-month-old plants (Figure 3C), probably
377 indicating a damage to PSII or photoinactivation caused by a decrease of the opened reaction
378 centers. The quantum yield of PSII values detected in 4-month-old plants were higher (some
379 significantly) than ones detected in 2-month-old plants (Figure 3D). No significant influence of
380 CHT treatment was recorded in F_v/F_m ratio and similarly occurred in ϕPSII value, compared to
381 untreated and only infected plants (CMV-TP) (Figures 3C and D, respectively).
382 SPAD meter measures the relative chlorophyll content by estimating the leaf greenness. Indeed,
383 chlorophyll reflects a green light, inducing this color in plants (Shi et al., 2018). Results indicated
384 no significant difference in SPAD readings of CMV-TP, compared to untreated plants, in the same
385 interval measurements. However, in 4-month-old plants, CMV-TP had a SPAD value lower than
386 that of untreated plants, reflecting the changed pigmentation responsible for the symptoms
387 displayed. Furthermore, our data indicated that CHT-TP showed a significant increase in
388 chlorophyll content, compared to untreated ones, in 2-month-old plants (Figure 4). Van et al. (2013)
389 also reported that CHT nanoparticles improved the content of chlorophylls as well as the uptake of
390 nitrogen and magnesium that constitute the chlorophyll chemical structure.
391 Phenols produced by plants vary in the defense response against environmental stresses (Sofo et al.,
392 2017). In our case, 60 h after CMV inoculation, foliar total phenolic content was not significantly
393 different between CMV-TP and untreated plants (Figure 5). The same result was obtained six days
394 after the inoculation of CMV-Y in tobacco plants (Ipper et al., 2008). Furthermore, the treatment
395 with CHT, both alone and before CMV inoculation (CHT-TP and CHT-CMV-TP, respectively),
396 caused a decrease of total phenols, compared to ones determined in only infected and untreated
397 plants (Figure 5). In agreement with our result, Coqueiro et al. (2011) assessed the effect of low
398 molecular weight CHT in tomato plants, then inoculated with *Xanthomonas gardneri* three days

399 after CHT treatment. They observed that the total phenolic compounds of the CHT-treated plants
400 increased starting from the second day after the inoculation of *Xanthomonas gardneri*, hence neither
401 before nor within 24 h after inoculation. Therefore, in our case, the absence of a CHT-conditioned
402 accumulation of phenolics as a response to CMV in CHT-CMV-TP may be due to the chosen
403 timing between CHT application and CMV inoculation (24 h) and/or between inoculation and
404 analysis (60 h).

405

406 **4.3 Expression analysis of defense-related genes**

407

408 The systemic acquired resistance (SAR) provides to the plant a long-lasting systemic resistance to
409 consecutive infections by many pathogens (Mou et al., 2003). The SAR involves plant responses,
410 such as the production of reactive oxygen species (ROS) and pathogenesis-related (PR) proteins, as
411 well as the lignification and cell wall reinforcement through the cell wall structural proteins cross-
412 linking (Pandey et al., 2017). More specifically, the CHT-induced resistance can enhance the
413 activities of defense-related enzymes, such as peroxidase, PAL, polyphenol oxidase, superoxide
414 dismutase and catalase (Xing et al., 2015). The induced systemic resistance (ISR) is triggered by
415 some bacteria and fungi and requires jasmonic acid (JA) and ethylene (ET). Differently, the SAR
416 requires salicylic acid (SA), exogenously applied (Mou et al., 2003) or endogenously produced.
417 To optimize the GrayNorm output for the molecular analysis, the four different experimental
418 conditions were divided into two groups (Figures 6 and 7). It was appropriate to compare the
419 expression of the assayed genes in CHT-TP and CHT-CMV-TP to untreated plants. Such
420 comparison denoted that CHT treatment causes an up-regulation of *CEVI-1*, *NPR1* and *PAL5*
421 expressions, whereas the increase of *PSY2* is only observed in even infected plants.
422 Particularly, peroxidases are enzymes that catalyze the hydrogen peroxide (H_2O_2) decomposition
423 oxidating many phenolic and non-phenolic substrates (Pandey et al., 2017). The implication of plant

peroxidases in processes, such as lignification, suberization, cell wall metabolism, defense against pathogens and ROS metabolism is well-known (Pandey et al., 2017). Although not statistically different, a strong increase in *CEVI-1* expression occurred in CMV-TP, compared to untreated plants (Figure 6A). Such finding is in accordance with the observation that at seven days post *Tomato mosaic virus* (ToMV) inoculation of tomato plants, *CEVI-1* expression was induced in leaves (Mayda et al., 2000). *CEVI-1* expression strong up-regulation could be associated with the cell wall reinforcement and the ROS content. Mayda et al. (2000) also reported that were able to induce *CEVI-1* expression neither incompatible interactions nor some infiltrated signal molecules. Compared to CMV-TP, the CHT treatment in CHT-CMV-TP seemed to limit the *CEVI-1* transcripts amount (Figure 7A), suggesting that CHT plays a role in the regulation of the ROS levels, thus controlling such CMV infection effect.

Cytosolic non-expressor of pathogenesis-related genes 1 (NPR1) regulates the salicylate- and jasmonate-dependent pathways cross-talk (Spoel et al., 2003). Moreover, in *Arabidopsis*, *Bacillus cereus* AR156-induced ISR to *Botrytis cinerea* required *NPR1* and JA/ET-signaling pathway (Nie et al., 2017). Interestingly, another study demonstrated that SAR induction by AR156 required *NPR1* and SA-signaling pathway (Niu et al., 2016). Wu et al. (2012) suggested that *Arabidopsis* NPR1 binds SA through cysteines$^{521/529}$ via copper. Just during SAR, NPR1 activates the PR gene expression (Mou et al., 2003). In our study, the expression of *NPR1* was analyzed as well, but no significant differences in the transcripts amount were detected (Figures 6B and 7B). However, *NPR1* expression was slightly up-regulated in CHT-TP and CHT-CMV-TP, compared to CMV-TP (Figure 7B) and untreated ones. This could indicate the CHT efficacy against CMV by triggering SAR-related defense responses in tomato plants. Jia et al. (2016) reported that CHT oligosaccharide pretreatment induced TMV resistance in *Arabidopsis* through the SA signalling pathway. An optimal low concentration (50 mg L^{-1}) applied one day before TMV inoculation was used.

448 Interestingly, Doares et al. (1995) observed an increase in the level of JA in leaves of excised
449 tomato plants after supplying CHT oligosaccharides.
450 Photosynthesis and photoprotection are processes involving plant carotenoids (Giorio et al., 2008).
451 The first biosynthetic step of carotenoids involves two molecules of geranylgeranyl pyrophosphate
452 (GGPP) and is catalyzed by the enzyme phytoene synthase (PSY), that is encoded by *PSY2* in
453 chloroplasts and *PSY1* of chromoplasts in tomato. From phytoene, sequential reactions differently
454 form lycopene and then cyclic carotenoids such as lutein, zeaxanthin and violaxanthin (Fraser and
455 Bramley, 2004; Giorio et al., 2008; Meléndez-Martínez et al., 2010). However, such two genes
456 encode PSY2 and PSY1, respectively (Giorio et al., 2008). In our case, *PSY2* expression was up-
457 regulated in CMV-TP, but such a result was not significant; On the whole, no significant difference
458 was observed in the *PSY2* transcript amount (Figures 6C and 7C). Interestingly, Ibdah et al. (2014)
459 found that CMV-Fny infection caused an increased phytoene content in *Nicotiana tabacum* L. cv.
460 Samsun NN roots; however, the carotenoid production was reduced because the enzyme phytoene
461 desaturase was down-regulated by CMV.
462 Additionally, phenylalanine ammonia lyase (PAL) converts the L-phenylalanine to ammonia and
463 trans-cinnamic acid. PAL-catalyzed reaction is the first in phenylpropanoid metabolism. Lee et al.
464 (1994) demonstrated that multiple initiation sites in *PAL5* allow the tomato plant to respond to
465 different environmental stimuli in a tissue-specific fashion. In our experiment, a significant increase
466 in *PAL5* expression occurred in CHT-TP and CHT-CMV-TP, compared to CMV-TP (Figure 7D).
467 Such a result is in accordance with Mejía-Teniente et al. (2013), who observed that after the first
468 CHT treatment in *Capsicum annuum* L., PAL activity as well as *pal* expression increased. No
469 significant difference was observed in *PAL5* expression level in CMV-TP, compared to untreated
470 plants (Figure 6D). Ogawa et al. (2006) found increased *PAL A* and *PAL B* transcripts as well as
471 PAL activity in TMV-infected (hypersensitive reaction lesion-bearing) tobacco leaves, suggesting
472 the phenylalanine pathway as the main route of SA synthesis. Compared to CMV-TP, the

473 significantly higher *PAL5* expression detected in CHT-CMV-TP (Figure 7D), suggests the
474 involvement of phenylpropanoid-derived products as lignin and SA.
475 The RNA silencing participates in the antiviral plant mechanism, though it is overcome by the
476 viruses encoding RNA silencing suppressors (Carr et al., 2010), such as the 2b protein of CMV.
477 Unfortunately, how virus infection is controlled in plants exhibiting SAR has not
478 been fully understood (Carr et al., 2010).

479

480 **5 Conclusions**

481

482 This paper reports the ability of chitosan as a preventive treatment able to elicit defense responses in
483 tomato plants against CMV-Fny infection. Chitosan was able to reduce the CMV titer and improved
484 the gas exchange of the infected plants. Furthermore, a SAR-related response induced by chitosan,
485 also by influencing the plant oxidative status, is hypotizable. Such findings represent a new and
486 additional piece of the puzzle depicting effective, sustainable and environmentally safe methods of
487 plant disease control. Further studies could clearly define the whole set of the resistance responses
488 triggered specifically in such host-pathogen-elicitor combination.

489

490 **Conflict of interest statement**

491 Declarations of interest: none.

492

493 **Funding**

This research did not receive any specific grant from funding agencies in the public, commercial, or not-for-profit sectors.

Acknowledgments

We gratefully thank Els Keunen, Stefanie De Smet, Rafaela Amaral dos Reis, Sophie Hendrix and Jana Deckers for their statistical and technical support.

References

Agrios, G.N., 1997. Plant Pathology, fourth ed. Academic Press, San Diego.

Anfoka, G.H., 2000. Benzo-(1,2,3)-thiadiazole-7-carbothioic acid *S*-methyl ester induces systemic resistance in tomato (*Lycopersicon esculentum*. Mill cv. Vollendung) to *Cucumber mosaic virus*. Crop Prot. 19, 401–405. https://doi.org/10.1016/S0261-2194(00)00031-4.

Carr, J.P., Lewsey, M.G., Palukaitis, P., 2010. Signaling in induced resistance, in: Carr, J.P., Loebenstein, G. (Eds.), Advances in Virus Research. Academic Press, Burlington, pp. 57–121.

Chirkov, S.N., Il'ina, A.V., Surgucheva, N.A., Letunova, E.V., Varitsev, Y.A., Tatarinova, N.Y., Varlamov, V.P., 2001. Effect of chitosan on systemic viral infection and some defense responses in potato plants. Russ. J. Plant Physiol. 48, 774–779. https://doi.org/10.1023/A:1012508625017.

Coqueiro, D.S.O., Maraschin, M., Di Piero, R.M., 2011. Chitosan reduces bacterial spot severity and acts in phenylpropanoid metabolism in tomato plants. J. Phytopathol. 159, 488–494. https://doi.org/10.1111/j.1439-0434.2011.01791.x.

Doares, S.H., Syrovets, T., Weiler, E.W., Ryan, C.A., 1995. Oligogalacturonides and chitosan activate plant defensive genes through the octadecanoid pathway. Proc. Natl. Acad. Sci. USA. 92, 4095–4098.

Edwardson, J.R., Christie, R.G., 1991. CRC Handbook of Viruses Infecting Legumes, CRC Press, Boca Raton.

Feliziani, E., Landi, L., Romanazzi, G., 2015. Preharvest treatments with chitosan and other alternatives to conventional fungicides to control postharvest decay of strawberry. Carbohydr. Polym. 132, 111–117. https://doi.org/10.1016/j.carbpol.2015.05.078.

Fraser, P.D., Bramley, P.M., 2004. The biosynthesis and nutritional uses of carotenoids. Prog. Lipid Res. 43, 228–265. https://doi.org/10.1016/j.plipres.2003.10.002.

542 Gallitelli, D., 2000. The ecology of *Cucumber mosaic virus* and sustainable agriculture. Virus Res.
543 71, 9–21. https://doi.org/10.1016/S0168-1702(00)00184-2.
544 Gallitelli, D., 1998. Present status of controlling *Cucumber mosaic virus*, in: Hadidi, A., Khetarpal,
545 R.K., Koganezawa, H. (Eds.), Plant Virus Disease Control. APS Press, St. Paul, pp. 507–523.
546 Giorio, G., Stigliani, A.L., D'Ambrosio, C., 2008. Phytoene synthase genes in tomato (*Solanum*
547 *lycopersicum* L.) - new data on the structures, the deduced amino acid sequences and the
548 expression patterns. FEBS J. 275, 527–535. https://doi.org/10.1111/j.1742-4658.2007.06219.x.
549 Hassan, O., Chang, T., 2017. Chitosan for eco-friendly control of plant disease. Asian J. Plant
550 Pathol. 11, 53−70. https://doi.org/10.3923/ajppaj.2017.53.70.
551 Ibdah, M., Dubey, N.K., Eizenberg, H., Dabour, Z., Abu-Nassar, J., Gal-On, A., Aly, R., 2014.
552 *Cucumber mosaic virus* as a carotenoid inhibitor reducing *Phelipanche aegyptiaca* infection in
553 tobacco plants. Plant Signal. Behav. 9, e972146. http://dx.doi.org/10.4161/psb.32096.
554 Ipper, N.S., Cho, S., Lee, S.H., Cho, J.M., Hur, J.H., Lim, C.K., 2008. Antiviral activity of the
555 exopolysaccharide produced by *Serratia* sp. strain Gsm01 against *Cucumber mosaic virus*. J.
556 Microbiol. Biotechnol. 18, 67–73.
557 Iriti, M., Picchi, V., Rossoni, M., Gomarasca, S., Ludwig, N., Gargano, M., Faoro, F., 2009.
558 Chitosan antitranspirant activity is due to abscisic acid-dependent stomatal closure. Environ.
559 Exp. Bot. 66, 493–500. https://doi.org/10.1016/j.envexpbot.2009.01.004.
560 Iriti, M., Varoni, E.M., 2015. Chitosan-induced antiviral activity and innate immunity in plants.
561 Environ. Sci. Pollut. Res. 22, 2935–2944. https://doi.org/10.1007/s11356-014-3571-7.
562 Jia, X., Meng, Q., Zeng, H., Wang, W., Yin, H., 2016. Chitosan oligosaccharide induces resistance
563 to *Tobacco mosaic virus* in *Arabidopsis* via the salicylic acid-mediated signalling pathway.
564 Sci. Rep. 6, 26144. https://doi.org/10.1038/srep26144.
565 Kumar, S., Chauhan, P.S., Agrawal, L., Raj, R., Srivastava, A., Gupta, S., Mishra, S.K., Yadav, S.,
566 Singh, P.C., Raj, S.K., Nautiyal, C.S., 2016. *Paenibacillus lentimorbus* inoculation enhances

tobacco growth and extenuates the virulence of *Cucumber mosaic virus*. PLoS One. 11, e0149980. https://doi.org/10.1371/journal.pone.0149980.

Kumaraswamy, R.V., Kumari, S., Choudhary, R.C., Pal, A., Raliya, R., Biswas, P., Saharan, V., 2018. Engineered chitosan based nanomaterials: bioactivities, mechanisms and perspectives in plant protection and growth. Int. J. Biol. Macromol. 113, 494–506. https://doi.org/10.1016/j.ijbiomac.2018.02.130.

Lee, S.W., Heinz, R., Robb, J., Nazar, R.N., 1994. Differential utilization of alternate initiation sites in a plant defense gene responding to environmental stimuli. Eur. J. Biochem. 226, 109–114. https://doi.org/10.1111/j.1432-1033.1994.0t109.x.

Liu, D., Jiao, S., Cheng, G., Li, X., Pei, Z., Pei, Y., Yin, H., Du, Y., 2018. Identification of chitosan oligosaccharides binding proteins from the plasma membrane of wheat leaf cell. Int. J. Biol. Macromol. 111, 1083–1090. https://doi.org/10.1016/j.ijbiomac.2018.01.113.

Liu, H., Du, Y., Wang, X., Sun, L., 2004. Chitosan kills bacteria through cell membrane damage. Int. J. Food Microbiol. 95, 147–155. https://doi.org/10.1016/j.ijfoodmicro.2004.01.022.

Malerba, M., Cerana, R., 2016. Chitosan effects on plant systems. Int. J. Mol. Sci. 17, 996. https://doi.org/10.3390/ijms17070996.

Marler, T.E., Mickelbart, M.V., Quitugua, R., 1993. Papaya ringspot virus influences net gas exchange of papaya leaves. HortScience. 28, 322–324.

Mayda, E., Marqués, C., Conejero, V., Vera, P., 2000. Expression of a pathogen-induced gene can be mimicked by auxin insensitivity. Mol. Plant Microbe Interact. 13, 23–31. https://doi.org/10.1094/MPMI.2000.13.1.23.

Mejía-Teniente, L., de Dalia Duran-Flores, F., Chapa-Oliver, A.M., Torres-Pacheco, I., Cruz-Hernández, A., González-Chavira, M.M., Ocampo-Velázquez, R.V., Guevara-González, R.G., 2013. Oxidative and molecular responses in *Capsicum annuum* L. after hydrogen peroxide, salicylic acid and chitosan foliar applications. Int. J. Mol. Sci. 14, 10178–10196.

https://doi.org/10.3390/ijms140510178.

Meléndez-Martínez, A.J., Fraser, P.D., Bramley, P.M., 2010. Accumulation of health promoting phytochemicals in wild relatives of tomato and their contribution to *in vitro* antioxidant activity. Phytochemistry. 71, 1104–1114. https://doi.org/10.1016/j.phytochem.2010.03.021.

Mou, Z., Fan, W., Dong, X., 2003. Inducers of plant systemic acquired resistance regulate NPR1 function through redox changes. Cell. 113, 935–944. https://doi.org/10.1016/S0092-8674(03)00429-X.

Murchie, E.H., Lawson, T., 2013. Chlorophyll fluorescence analysis: a guide to good practice and understanding some new applications. J. Exp. Bot. 64, 3983–3998. https://doi.org/10.1093/jxb/ert208.

Nagorskaya, V., Reunov, A., Lapshina, L., Davydova, V., Yermak, I., 2014. Effect of chitosan on *Tobacco mosaic virus* (TMV) accumulation, hydrolase activity, and morphological abnormalities of the viral particles in leaves of *N. tabacum* L. cv. Samsun. Virol. Sin. 29, 250–256. https://doi.org/10.1007/s12250-014-3452-8.

Nie, P., Li, X., Wang, S., Guo, J., Zhao, H., Niu, D., 2017. Induced systemic resistance against *Botrytis cinerea* by *Bacillus cereus* AR156 through a JA/ET- and *NPR1*-dependent signaling pathway and activates PAMP-triggered immunity in *Arabidopsis*. Front. Plant Sci. 8, 238. https://doi.org/10.3389/fpls.2017.00238.

Niu, D., Wang, X., Wang, Y., Song, X., Wang, J., Guo, J., Zhao, H., 2016. *Bacillus cereus* AR156 activates PAMP-triggered immunity and induces a systemic acquired resistance through a *NPR1*-and SA-dependent signaling pathway. Biochem. Biophys. Res. Commun. 469, 120–125. https://doi.org/ 10.1016/j.bbrc.2015.11.081.

Ogawa, D., Nakajima, N., Seo, S., Mitsuhara, I., Kamada, H., Ohashi, Y., 2006. The phenylalanine pathway is the main route of salicylic acid biosynthesis in *Tobacco mosaic virus*-infected tobacco leaves. Plant Biotechnol. 23, 395–398.

https://doi.org/10.5511/plantbiotechnology.23.395.

Pandey, V.P., Awasthi, M., Singh, S., Tiwari, S., Dwivedi, U.N., 2017. A comprehensive review on function and application of plant peroxidases. Biochem. Anal. Biochem. 6, 308. https://doi.org/10.4172/2161-1009.1000308.

Petutschnig, E.K., Jones, A.M.E., Serazetdinova, L., Lipka, U., Lipka, V., 2010. The lysin motif receptor-like kinase (LysM-RLK) CERK1 is a major chitin-binding protein in *Arabidopsis thaliana* and subject to chitin-induced phosphorylation. J. Biol. Chem. 285, 28902–28911. https://doi.org/10.1074/jbc.M110.116657.

Povero, G., Loreti, E., Pucciariello, C., Santaniello, A., Di Tommaso, D., Di Tommaso, G., Kapetis, D., Zolezzi, F., Piaggesi, A., Perata, P., 2011. Transcript profiling of chitosan-treated *Arabidopsis* seedlings. J. Plant Res. 124, 619–629. https://doi.org/10.1007/s10265-010-0399-1.

Salachna, P., Byczyńska, A., Jeziorska, I., Udycz, E., 2017. Plant growth of *Verbena bonariensis* L. after chitosan, gellan gum or iota-carrageenan foliar applications. World Sci. News 62, 111−123.

Sharif, R., Mujtaba, M., Ur Rahman, M., Shalmani, A., Ahmad, H., Anwar, T., Tianchan, D., Wang, X., 2018. The multifunctional role of chitosan in horticultural crops; a review. Molecules 23, 872. https://doi.org/10.3390/molecules23040872.

Shi, J., Yu, L., Song, B., 2018. Proteomics analysis of Xiangcaoliusuobingmi-treated *Capsicum annuum* L. infected with *Cucumber mosaic virus.* Pest. Biochem. Physiol. 149, 113–122. https://doi.org/10.1016/j.pestbp.2018.06.008.

Sivakumar, D., Bill, M., Korsten, L., Thompson, K., 2016. Integrated application of chitosan coating with different postharvest treatments in the control of postharvest decay and maintenance of overall fruit quality, in: Bautista-Baños, S., Romanazzi, G., Jiménez-Aparicio, A. (Eds.), Chitosan in the Preservation of Agricultural Commodities. Academic Press, Cambridge, pp. 127–153.

642 Sofo, A., Bochicchio, R., Amato, M., Rendina, N., Vitti, A., Nuzzaci, M., Altamura, M.M., Falasca,
643 G., Della Rovere, F., Scopa, A., 2017. Plant architecture, auxin homeostasis and phenol
644 content in *Arabidopsis thaliana* grown in cadmium- and zinc-enriched media. J. Plant Physiol.
645 216, 174–180. https://doi.org/10.1016/j.jplph.2017.06.008.
646 Spoel, S.H., Koornneef, A., Claessens, S.M.C., Korzelius, J.P., Van Pelt, J.A., Mueller, M.J.,
647 Buchala, A.J., Métraux, J.P., Brown, R., Kazan, K., Van Loon, L.C., Dong, X., Pieterse,
648 C.M.J., 2003. NPR1 modulates cross-talk between salicylate- and jasmonate-dependent
649 defense pathways through a novel function in the cytosol. Plant Cell. 15, 760–770.
650 https://doi.org/10.1105/tpc.009159.
651 Van, S.N., Minh, H.D., Anh, D.N., 2013. Study on chitosan nanoparticles on biophysical
652 characteristics and growth of Robusta coffee in green house. Biocatal. Agric. Biotechnol. 2,
653 289–294. https://doi.org/10.1016/j.bcab.2013.06.001.
654 Vitti, A., La Monaca, E., Sofo, A., Scopa, A., Cuypers, A., Nuzzaci, M., 2015. Beneficial effects of
655 *Trichoderma harzianum* T-22 in tomato seedlings infected by *Cucumber mosaic virus* (CMV).
656 BioControl. 60, 135–147. https://doi.org/10.1007/s10526-014-9626-3.
657 Vitti, A., Pellegrini, E., Nali, C., Lovelli, S., Sofo, A., Valerio, M., Scopa, A., Nuzzaci, M., 2016.
658 *Trichoderma harzianum* T-22 induces systemic resistance in tomato infected by *Cucumber*
659 *mosaic virus*. Front. Plant Sci. 7, 1520. https://doi.org/10.3389/fpls.2016.01520.
660 Wu, Y., Zhang, D., Chu, J.Y., Boyle, P., Wang, Y., Brindle, I.D., De Luca, V., Després, C., 2012.
661 The *Arabidopsis* NPR1 protein is a receptor for the plant defense hormone salicylic acid. Cell
662 Rep. 1, 639–647. https://doi.org/10.1016/j.celrep.2012.05.008.
663 Xing, K., Zhu, X., Peng, X., Qin, S., 2015. Chitosan antimicrobial and eliciting properties for pest
664 control in agriculture: a review. Agron. Sustain. Dev. 35, 569–588.
665 https://doi.org/10.1007/s13593-014-0252-3.
666 Zhang, D., Wang, H., Hu, Y., Liu, Y., 2015. Chitosan controls postharvest decay on cherry tomato

fruit possibly via the mitogen-activated protein kinase signaling pathway. J. Agric. Food Chem. 63, 7399–7404. https://doi.org/10.1021/acs.jafc.5b01566.

Zhao, J., Zhang, X., Hong, Y., Liu, Y., 2016. Chloroplast in plant-virus interaction. Front. Microbiol. 7, 1565. https://doi.org/10.3389/fmicb.2016.01565.

692 Figure 1. Phenotypical observations of symptoms induced by *Cucumber mosaic virus* (CMV) 20 days and 11 days after
693 CMV inoculation of representative A) *Solanum lycopersicum* var. *cerasiforme* and B) *Nicotiana tabacum* cv Xanthi
694 plants, respectively. Four different experimental conditions: untreated plants; plants inoculated with CMV (CMV-TP);
695 plants treated with CHT (CHT-TP); plants treated with CHT and then inoculated with CMV 24 h after CHT treatment
696 (CHT-CMV-TP).
697

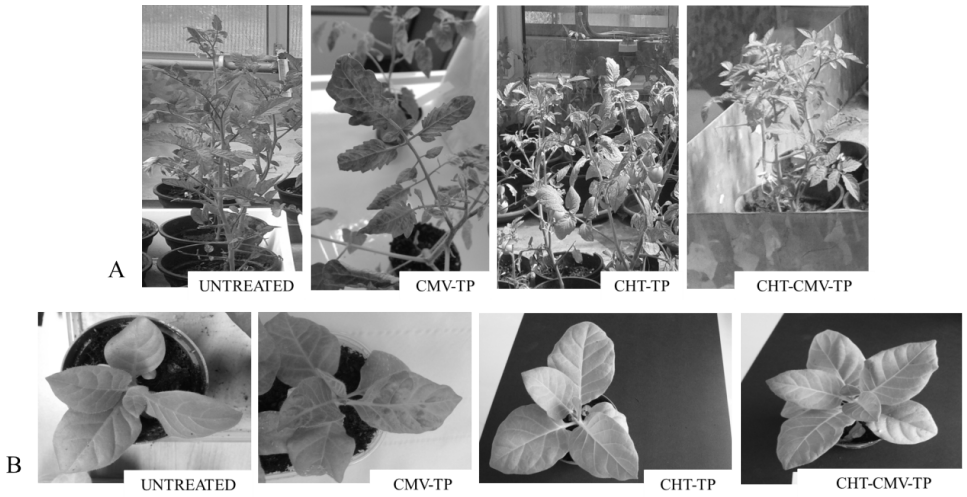

698
699

Figure 2. *Cucumber mosaic virus* (CMV) load 20 days (light grey bars) and 90 days (dark grey bars) after CMV inoculation of tomato plants. Mean values ($n = 6$) are represented. Standard deviations are represented by bars. Significant differences ($P \leq 0.05$) among treatments and time are indicated by different letters, according to non-parametric two-way ANOVA. Four different experimental conditions: untreated plants; plants inoculated with CMV (CMV-TP); plants treated with CHT (CHT-TP); plants treated with CHT and then inoculated with CMV 24 h after CHT treatment (CHT-CMV-TP).

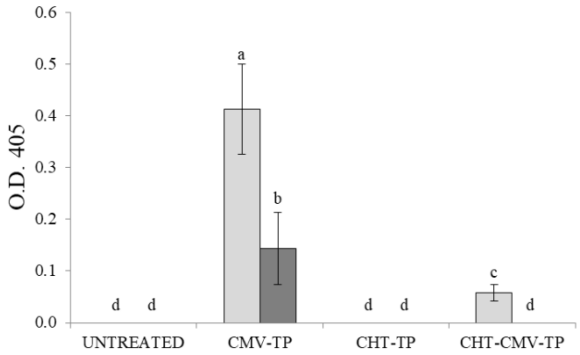

Figure 3. Gas exchange and chlorophyll fluorescence determinations. A) Photosynthetic activity (A), B) stomatal conductance to water vapor (g_s), C) maximal quantum yield of PSII (F_v/F_m) and D) quantum yield of PSII (ϕPSII), measured in 2- (light grey bars) and 4-month-old (dark grey bars) tomato plants. Mean values ($n \geq 6$ for gas exchange; $n = 4$ for chlorophyll fluorescence) are represented. Standard deviations are represented by bars. Significant differences ($P \leq 0.05$) among treatments and time are indicated by different letters, according to parametric and non-parametric (g_s) two-way ANOVA. Four different experimental conditions: untreated plants; plants inoculated with CMV (CMV-TP); plants treated with CHT (CHT-TP); plants treated with CHT and then inoculated with CMV 24 h after CHT treatment (CHT-CMV-TP).

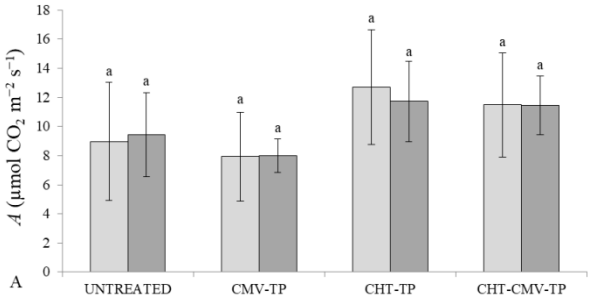

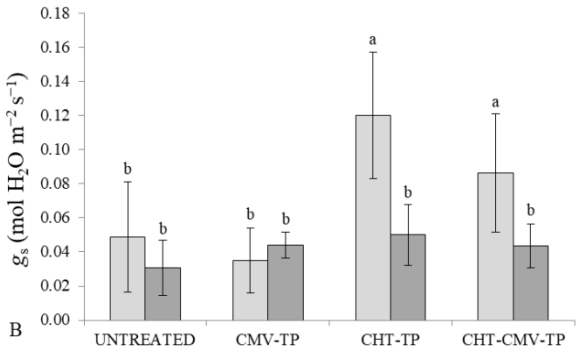

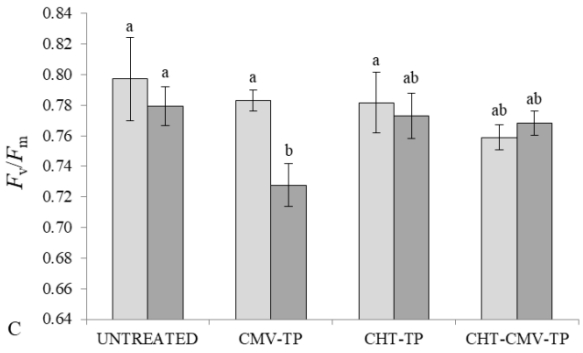

C

719

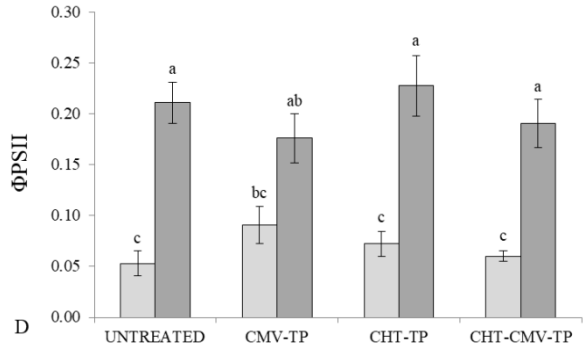

D

720

721

Figure 4. Chlorophyll content (SPAD) measured in 2- (light grey bars) and 4-month-old (dark grey bars) tomato plants. Mean values ($n = 6$) are represented. Standard deviations are represented by bars. Significant differences ($P \leq 0.05$) among treatments and time are indicated by different letters, according to non-parametric two-way ANOVA. Four different experimental conditions: untreated plants; plants inoculated with CMV (CMV-TP); plants treated with CHT (CHT-TP); plants treated with CHT and then inoculated with CMV 24 h after CHT treatment (CHT-CMV-TP).

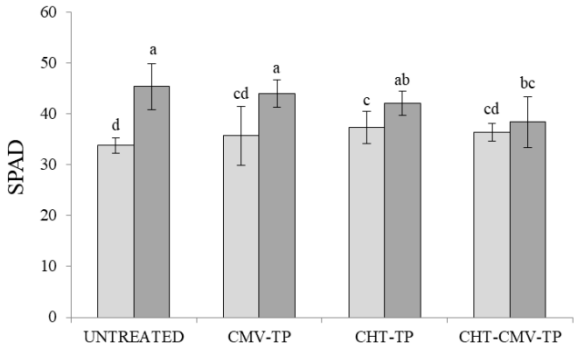

Figure 5. Total phenolic content of tomato leaves. Mean values ($n = 4$) are represented. Standard deviations are represented by bars. Significant differences ($P \leq 0.05$) among treatments are indicated by different letters, according to non-parametric one-way ANOVA. Four different experimental conditions: untreated plants; plants inoculated with CMV (CMV-TP); plants treated with CHT (CHT-TP); plants treated with CHT and then inoculated with CMV 24 h after CHT treatment (CHT-CMV-TP).

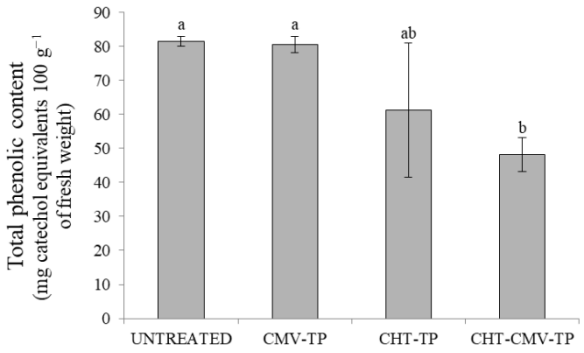

Figure 6. Genes expression in CMV-TP relatively expressed to the Untreated tomato plants. A) peroxidase (*CEVI-1*), B) non-expressor of pathogenesis-related genes 1 (*NPR1*), C) phytoene synthase 2 (*PSY2*) and D) phenylalanine ammonia lyase (*PAL5*). Mean values ($n = 4$) are represented. Standard errors are represented by bars. Significant differences ($P \leq 0.05$) among treatments are indicated by different letters, according to parametric one-way ANOVA. Two different experimental conditions: untreated plants; plants inoculated with CMV (CMV-TP).

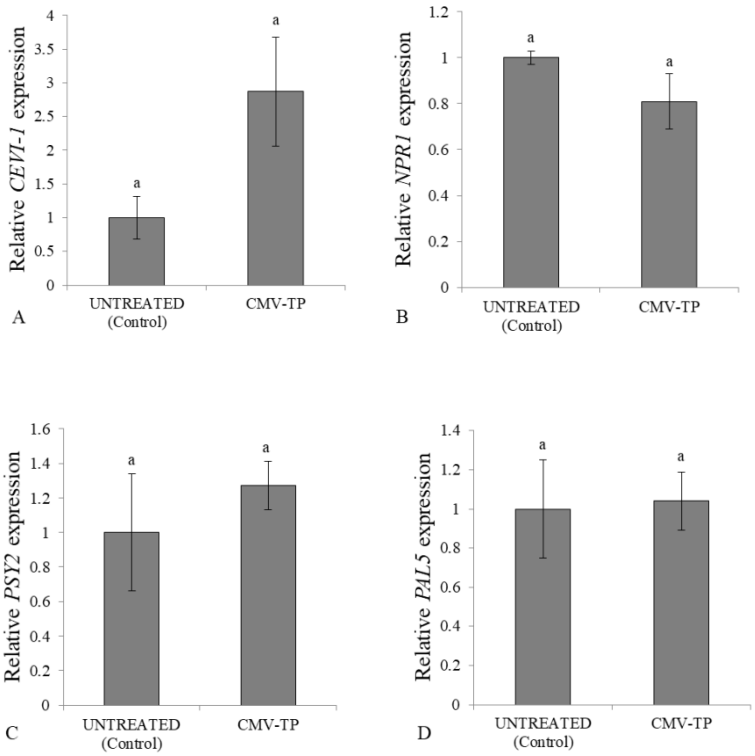

Figure 7. Genes expression in CHT-TP and CHT-CMV-TP relatively expressed to the CMV-TP (tomato plants). A) peroxidase (*CEVI-1*), B) non-expressor of pathogenesis-related genes 1 (*NPR1*), C) phytoene synthase 2 (*PSY2*) and D) phenylalanine ammonia lyase (*PAL5*). Mean values ($n = 4$) are represented. Standard errors are represented by bars. Significant differences ($P \leq 0.05$) among treatments are indicated by different letters, according to parametric one-way ANOVA. Three different experimental conditions: plants inoculated with CMV (CMV-TP); plants treated with CHT (CHT-TP); plants treated with CHT and then inoculated with CMV 24 h after CHT treatment (CHT-CMV-TP).